AD-A181 642 EXPERIMENTAL RESULTS FROM RAILGUN FIRINGS INVOLVING MAGNETIC FLUX PROBES(U) MATERIALS RESEARCH LABS ASCOT VALE (AUSTRALIA) V KOWALENKO DEC 86 MRL-TN-509 1/1

UNCLASSIFIED F/G 20/3 NL

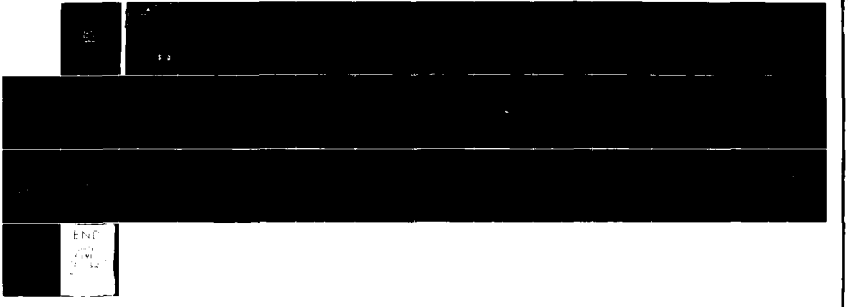

END

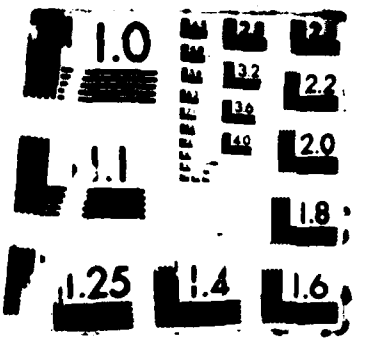
1.0
1.1
1.25
1.4
1.6
1.8
2.0
2.2

MRL-TN-509

AR-005-103

DEPARTMENT OF DEFENCE

DEFENCE SCIENCE AND TECHNOLOGY ORGANISATION

MATERIALS RESEARCH LABORATORIES

MELBOURNE, VICTORIA

TECHNICAL NOTE

MRL-TN-509

EXPERIMENTAL RESULTS FROM RAILGUN FIRINGS INVOLVING MAGNETIC FLUX PROBES

V. Kowalenko

Approved for Public Release

DECEMBER 1986

DEPARTMENT OF DEFENCE
MATERIALS RESEARCH LABORATORIES

TECHNICAL NOTE

MRL-TN-509

EXPERIMENTAL RESULTS FROM RAILGUN FIRINGS INVOLVING MAGNETIC FLUX PROBES

V. Kowalenko

ABSTRACT

In the Magnetic RAPID Plasma Intensity Profiles (MRAP) series of railgun firings, the voltages induced in small solenoidal probes mounted in different positions and orientations along the barrel were measured to gain a better understanding of the current density and magnetic field in a plasma armature. A summary of the results obtained from the probes is presented in this technical note. In addition, results obtained from the image analyses of streak films are presented together with some of the diagnostic records taken during the series.

Approved for Public Release

POSTAL ADDRESS: Director, Materials Research Laboratories
P.O. Box 50, Ascot Vale, Victoria 3032, Australia

SECURITY CLASSIFICATION OF THIS PAGE UNCLASSIFIED AD-A181-642

DOCUMENT CONTROL DATA SHEET

REPORT NO.	AR NO.	REPORT SECURITY CLASSIFICATION
MRL-TN-509	AR-005-105	Unclassified

TITLE

Experimental results from railgun firings involving magnetic flux probes

AUTHOR(S)

V. Kowalenko

CORPORATE AUTHOR

Materials Research Laboratories
P.O. Box 50,
Ascot Vale, Victoria 3032

REPORT DATE	TASK NO.	SPONSOR
December 1986	DST 82/212	DSTO

FILE NO.	REFERENCES	PAGES
G6/4/8-3211	6	40

CLASSIFICATION/LIMITATION REVIEW DATE

CLASSIFICATION/RELEASE AUTHORITY
Superintendent, MRL
Physics Division

SECONDARY DISTRIBUTION

Approved for Public Release

ANNOUNCEMENT

Announcement of this report is unlimited

KEYWORDS

Railgun Accelerators
Electromagnetic Launchers
Current Distribution
Magnetic Fields
Plasma Armature

COSATI GROUPS 2009 1906

ABSTRACT

In the Magnetic RAPID Plasma Intensity Profiles (MRAP) series of railgun firings, the voltages induced in small solenoidal probes mounted in different positions and orientations along the barrel were measured to gain a better understanding of the current density and magnetic field in a plasma armature. A summary of the results obtained from the probes is presented in this technical note. In addition, results obtained from the image analyses of streak films are presented together with some of the diagnostic records taken during the series.

CONTENTS

EXPERIMENTAL RESULTS FROM RAILGUN FIRINGS

INVOLVING MAGNETIC FLUX PROBES

1. INTRODUCTION

The Lorentz force acting on the plasma-projectile system in an electromagnetic launcher can only be evaluated if the current density ($\underset{\sim}{j}$) and the magnetic field ($\underset{\sim}{B}$) in the plasma armature are known. The magnetic field in the plasma armature is determined from the current distributions/densities in the rails and in the plasma. The current densities are found by solving the current diffusion equation with the appropriate boundary conditions at the rail surfaces and at the rail-plasma boundary. However, for the railgun these boundary conditions are not yet known and thus solutions to the current diffusion equation cannot be obtained.

An alternative approach, which can be used to evaluate the Lorentz force, is to specify possible models for the current distributions in the rails and in the plasma armature and then calculate the magnetic field in the plasma armature using these models. The Lorentz force is obtained by integrating the vector cross-product of $\underset{\sim}{j}$ and $\underset{\sim}{B}$ over the volume of the plasma armature. The accuracy of this second approach depends, of course, on the accuracy of the models for the current distributions. Experiments must be designed to check the current distribution models.

The magnetic field at any point P in the vicinity of the rails can be obtained from the Biot-Savart law provided the current distribution is quasi-stationary. The magnetic flux of a tiny solenoid probe or coil placed at point P is found using the component of the magnetic field pointing in the direction of the probe's axis of orientation. Differentiating the magnetic flux with respect to time yields the induced electromotive force (emf) for the probe, which can then be compared with the experimental measurements obtained by the probe during a railgun firing.

A series of nine railgun firings known as the Magnetic RAPID Plasma Intensity Profiles (MRAP) series was conducted in 1985 to measure the induced

emfs of solenoidal probes in different orientations at various positions along the gun-barrel during each firing. RAPID [1] is an acronym for a type of railgun used at MRL and means 'Railgun Armature Plasma Investigation Device'. In this technical note experimental results obtained from the MRAP series are presented.

The theoretical expressions derived for the induced emf of each probe are dependent on the railgun current, projectile displacement and plasma length as functions of time. In order to obtain accurate experimental data on the plasma length and projectile displacement as functions of time, light intensity profiles of the plasma armature were produced using streak films and an image analysis system at MRL.

The contents of this technical note are arranged as follows. In Section 2, the aims of the MRAP series are briefly stated whilst in Section 3, the experimental details are presented. Experimental results obtained from the series appear in Section 4 followed by a brief conclusion in Section 5.

2. AIMS OF THE SERIES

The aims of the MRAP series were:

(1) to gain further knowledge of the current distribution and magnetic field in the plasma armature,

(2) to compare theoretical predictions of the induced emf of various probes using simple models for the current distributions in the rails and in the plasma with the experimental results obtained from railgun firings,

(3) to conduct image analyses of the streak films to obtain more accurate position-time results than had previously been obtained,

(4) to obtain more accurate and more numerous data on plasma length as a function of time from the image analysis of the streak films, and

(5) to relate any possible differences between the theoretical predictions and the experimental results with possible anomalous behaviour appearing on the streak films.

In this technical note no comparison of the experimental results with theoretical predictions is presented. As mentioned previously, only the experimental results obtained from the series are presented.

3. EXPERIMENTAL DETAILS

The power source for the RAPID railgun [1] used in the MRAP series consisted of a 2.0 mF capacitor bank connected via a spark-gap switch to a 6.3 μH storage inductor. For each firing the capacitor bank was charged to 6.00 ± 0.03 kV. Crowbarring of the capacitor bank occurred about 200 μs after shot-start. The duration of a firing in the MRAP series was approximately 750 μs.

The magnetic probes used in the MRAP series had 10 turns each, were mounted in the insulating wall of the RAPID gun-body and were approximately 5 mm in diameter and 1 mm in length. The orientation axes of the probes were either parallel to the direction of projectile motion (longitudinal), parallel to the direction of the bore-height (vertical) or parallel to the direction of the bore-width (transverse). Because the induced emf of a transverse probe was calculated to be small and therefore not significant, only one transverse probe situated 413 mm from the breech with its orientation-axis 14 mm above the centre of the railgun bore was used. Measurements by this probe were only recorded in the fifth firing of the series (MRAP05). Vertical probes were placed 14 mm above the bore's centre and were situated 185, 335 and 435 mm from the breech. The longitudinal probes were situated in pairs with their axes of orientation 15 and 29 mm above the centre of the bore at 210, 360 and 460 mm from the breech as shown in Figure 1. The longitudinal and vertical probes were placed at the various positions to observe possible differences occurring in the induced emf during each firing. In addition, they were placed as close as possible to the bore so that the greatest possible rate of change in the magnetic flux would be recorded.

The probes situated nearest the breech are called breech coils (designated BC in Figure 1) whilst those situated nearest the muzzle are called muzzle coils (MC). The remaining central coils are designated CC. Vertical probes are designated in Figure 1 by the coils ending with a "1" such as BC1, CC1 and MC1. Longitudinal probes are designated by a "2" or a "3". The transverse probe is designated as MCT in Figure 1.

Pieces of aluminium foil weighing about 0.012 g were used to generate the plasma armatures in the MRAP series. Before each firing the aluminium foil was glued to the back of a polycarbonate projectile, which was placed 47 mm from the closed breech. The polycarbonate projectiles weighed approximately 0.40 g and had the dimensions of the bore cross-section (6 x 8 mm) and a length of 8 mm. The rails were 8 mm apart and were 0.5 m in length with a cross-section of 12 x 12 mm. As in the RAPID Plasma Intensity Profiles (RPIP) series [2], the rails were made of a copper-cadmium alloy.

The muzzle voltage and railgun current were recorded as functions of time on transient recorders in all of the MRAP firings. Due to a shortage of available channels on the transient recorders, the breech voltage was not recorded on the single firing when the transverse muzzle coil was operational. Because of doubts expressed in a previous report [2], the transient recorders measuring the railgun current were recalibrated before conducting the experiments. The new calibration factor is 1.08 ± 0.02 MA/V

which differs from the previous value of 0.92 ± 0.10 MA/V reported in Reference [3].

Light intensity profiles of the plasma armature were obtained from the streak films of a high speed CINE camera using an image analyser. Because position markers placed at 53, 200 and 350 mm were easily identified on the plasma intensity profiles, the position and length of the plasma armature during acceleration could be determined.

There were some other differences in experimental procedure between the RPIP and MRAP series. In MRAP07 and MRAP08 a transient recorder (IWATSU DM 7100) was used to measure the voltage across the crowbar switch. To minimise the effects of plasma leakage and arcing ahead of the projectile which appeared frequently in the RPIP series [2,4], the rear of each projectile used in the MRAP series was hollowed out. This meant that polycarbonate material was removed from the rear face of the projectile to a depth of about 1 mm leaving a thin skirt around the outer edges to give improved obturation. Finally, the time-of-arrival records were obtained using a different system of detectors to that employed in the RPIP series. In the MRAP series the system consisted of a muzzle flash detector, a pencil-lead-break situated 10 cm from the muzzle. two laser screens situated 50 and 75 cm from the lead-break and a breakscreen attached to a catch-tank, which was situated 110 cm from the muzzle. Unfortunately, this system was less reliable than the system used in the RPIP series.

4. EXPERIMENTAL RESULTS

4.1 Time-of-Arrival Records

Two examples of the time-of-arrival records obtained in the MRAP series are shown in Figures 2 and 3. In both figures the appearance of the marker indicates triggering of the transient recorder. In MRAP09 (Figure 3), the polarity was reversed accidentally. The vertical line crossing the time axis towards the end of the record in Figure 2 indicates the arrival time of the projectile at the catch-tank. This line does not appear in Figure 3 because the projectile either did not arrive before the transient recorder stopped measuring or it missed the breakscreen completely. It should be noted, however, that the vertical line crossing the time axis appears on all of the other time-of-arrival records except for MRAP04 and MRAP06. Time-of-arrival records were not obtained in these firings because the recording instrumentation failed to trigger.

In Figure 2, the time interval between the marker and the projectile's arrival time at the catch tank is 1.63×10^3 μs. The small peak about 1 mm or 12 μs from the marker corresponds to shot-start. The time interval between the first minimum about 5.5×10^2 μs after shot-start and the arrival time at the catch-tank is 1.10×10^3 μs. This minimum is supposed to correspond to the arrival time when the projectile broke the pencil-lead.

Hence the projectile's exit velocity is found to be 9.1×10^2 m/s, which is a value below the most successful firing of the RPIP series even though the initial input energy for the MRAP series was greater than the input energy for the RPIP series by 20 percent. In Table 2, the duration of MRAP08 obtained from the muzzle voltage record is given as 6.6×10^2 μs. A time of 6.6×10^2 μs from shot-start falls in the region of noise past the second minimum in Figure 2. Thus the minima on the time-of-arrival record in Figure 2 cannot be used to determine the exit velocity of the projectile. For the same reason the minima on the other time-of-arrival records cannot be used to determine the exit velocity.

In Table 2, estimates of the projectile exit velocities were obtained by subtracting the duration of the firing from the time interval between shot-start and the arrival time at the catch-tank and then dividing this result into the distance between the muzzle and the catch-tank (1.1 m). Included also in Table 2 are observations of the streak film, which provide details about the behaviour of the plasma armature. This behaviour is listed in Table 2 because it might have affected the accuracy of the estimates for the exit velocities.

4.2 Image Analysis Results

Since displacement and time correspond respectively to the horizontal and vertical directions on a streak film, plasma intensity profiles yielding the length and displacement of the plasma armature were obtained by scanning across a screen image of the streak film at different vertical positions along the film. Four examples of plasma intensity profiles are shown in Figures 4,5,6 and 7. In these figures the number of pixel positions horizontally across the image is referred to as the position co-ordinate. A decreasing intensity number indicates a greater light intensity emanating from the plasma. The plasma temperature is assumed to be higher for decreasing intensity number.

In MRAP02 the time calibration was facilitated by timing markers appearing at 100 μs intervals on the streak film. However, in the other MRAP firings these timing markers did not appear on the film due to equipment failure. The time was calibrated by determining the initial and exit positions of the projectile and then assigning the duration of the firing to the corresponding vertical distance between the projectile positions.

For each streak film three distinct screen images were produced. The horizontal axis of each image was calibrated by finding an appropriate intensity profile with two position markers on it. Position markers were easily identified on the light intensity profiles by a sudden increase in intensity number. Such an increase occurs at position co-ordinate 232 in Figure 4, which represents the position marker situated 53 mm from the breech. Since the distance between markers was known, the number of pixels per mm of gun barrel was found. This calibration factor was then used to determine the position of the leading edge of the plasma armature and the plasma length.

An intensity number of 50 was chosen for determining the plasma length of each intensity profile because the plasma light intensity for numbers below 50 appeared on the streak photograph whereas those above 50 did not appear. In some cases, eg. Figure 4, the position markers affected length estimates. When this occurred, the intensity profile was smoothed by disregarding the marker and the length estimate was then determined by measuring the interception distance for an intensity number equal to 50.

In MRAP05, length estimates were greatly affected by substantial plasma leakage. Figure 5 shows the light intensity profile for MRAP05 about 2.1×10^2 μs after shot-start. In this figure the plasma armature is distinguishable from plasma leakage because a gap in intensity occurs between position co-ordinates 210 and 220. However, at other times it is difficult to separate the two effects. For instance, in Figure 6 which shows the intensity profile for MRAP05 about 3.7×10^2 μs after shot-start the plasma length could be given by either the interception distance to point 1 or to point 2. In fact, plasma leakage may have occurred as far back as point 3 in the figure. Thus some very large values for the plasma length were obtained for MRAP05. Under these circumstances the plasma length results may not be valid.

Because very little plasma leakage occurred in MRAP08, the plasma lengths for this firing were significantly smaller than the plasma lengths for MRAP02 and MRAP05. However, uncertainties in the length results arose early in MRAP08. Light from the rear of the plasma armature exposed the edge of a sprocket hole on the film and this produced a sudden decrease in intensity number as shown in Figure 7. The light exposure behind the plasma armature in Figure 7 was neglected but in some of the earlier intensity profiles the separation between the plasma and the exposure at the edge of the sprocket had not occurred. Hence the length results early in MRAP08 may not be indicative of the actual plasma length.

The results of the image analyses for MRAP02, MRAP05 and MRAP08 appear in Tables 3,4 and 5 respectively. Included in these tables are the results for the position of the leading edge of the plasma armature for an intensity number equal to 50.

The graphs of the displacement-time results for MRAP02, MRAP05 and MRAP08 are shown without error bars in Figure 8. As can be seen, the displacement-time curve for the plasma front between $t = 160$ μs and $t = 400$ μs in MRAP05 is more erratic and greater than the displacement-time curves for the other two firings because of the severe plasma leakage, which occurred in MRAP05. The displacement-time curve for MRAP05 is therefore not representative of the projectile displacement. The displacement-time curves for MRAP02 and MRAP08 can be regarded as being close to the projectile displacement-time curves because plasma leakage was not significant in these firings. By using the GRAPH computer program.[5], the quadratic curve of best fit for MRAP02 was found to be:

$$x(t) = (6.7 \pm 0.3) \times 10^5 \, t^2 + (1.5 \pm 0.2) \times 10^2 \, t + (1.3 \pm 0.4) \times 10^{-2} \qquad (1)$$

where x is in metres and t is in seconds. For MRAP08, the quadratic curve of best fit was found to be:

$$x(t) = (7.5 \pm 0.2) \times 10^{5}\ t^{2} + (1.5 \pm 0.2) \times 10^{2}\ t + (2 \pm 3) \times 10^{-3} \qquad (2)$$

Differentiating equation (1) with respect to time and setting the time equal to the duration of MRAP02 (see Table 2) gives a value of $(1.1 \pm 0.1) \times 10^{3}$ m/s for the exit velocity of the projectile. The projectile's exit velocity for MRAP08 is determined in the same manner using equation (2) and is found to be $(1.1 \pm 0.1) \times 10^{3}$ m/s. From equation (1) the acceleration of the projectile ranged between 12.8×10^{5} and 14.0×10^{5} m/s^{2} whilst from equation (2) it ranged between 14.6×10^{5} and 15.4×10^{5} m/s^{2}.

The graphs of the plasma armature length versus time for MRAP02, MRAP05 and MRAP08 are shown without error bars in Figure 9. As expected, the plasma length for MRAP05 is significantly larger and more erratic than the plasma lengths for MRAP02 and MRAP08. On the given scale it can be seen that the plasma armature length for MRAP02 is almost constant for $t > 200\ \mu s$. In MRAP08 the plasma length is almost constant between $t = 120\ \mu s$ and $t = 320\ \mu s$. For $t > 320\ \mu s$, the plasma length decreases marginally until $t = 480\ \mu s$. The plasma length then increases till shot-out, indicating that the plasma armature was not well-behaved late in MRAP08.

4.3 Current-time Records

Current-time records were obtained from a transient recorder via an RC integrator connected to a Rogowski belt. The current-time record for MRAP08 is shown in Figure 10. This record agrees closely with all other current-time records.

The value of the peak current in Figure 10 is found to be $(8.8 \pm 0.2) \times 10^{4}$ A using the calibration factor of $(1.08 \pm 0.02) \times 10^{6}$ A/V. The energy in the storage inductor at peak current is then found to be $(2.4 \pm 0.2) \times 10^{4}$ J, which is approximately thirty percent less than the initial input energy. Some of this thirty percent energy difference is explained as energy lost due to resistive heating in the railgun circuit while the remaining energy is lost in exploding the wire across the switch gap and in creating the plasma armature. For more details concerning energy loss early in a railgun firing, the reader is referred to References [2,6].

4.4 Probe Measurements

The induced emfs of the vertical probes situated 185, 335 and 435mm from the breech are shown in Figures 11, 12 and 13 respectively. These figures show that the induced emf firstly increased and then decreased over the duration of measurement, which ranged between 60 and 90 μs. The maximum recorded voltage was different for each probe and also varied between

experiments. It was generally between 3.0 and 4.5 V. However, in some cases (Figure 12), the maximum voltage went off scale and thus the record was truncated. Both the duration of measurement and the maximum voltage are influenced by the current in the railgun circuit, the velocity of the plasma-projectile system and the length of the plasma armature.

The induced emf of the vertical probe situated 335 mm from the breech for MRAP02 was different from the other records and is shown in Figure 14. Although not established, the author believes that plasma breakup or disruption might have been responsible for this anomalous record. Light intensity gradients associated with plasma breakup were not observed on the plasma profiles for MRAP02 because the film might have been over-exposed.

The induced emfs recorded by longitudinal probes for some of the MRAP firings are presented in Figures 15 to 18. Figure 15 resembles very closely the theoretical predictions for the induced emf assuming that the plasma armature's current distribution is uniform. Figure 16 is also similar but indicates that the plasma armature was not as well-behaved as in Figure 15. In Figure 17, the induced emf has deviated considerably from the result for a well-behaved plasma armature (Figure 15). The peak emfs are also much lower than the peak emfs in Figure 15 presumably because the railgun current is no longer as high near the muzzle as it was at 210 mm from the breech. The induced emf of the central vertical probe for MRAP02 (Figure 18) is significantly different from the other longitudinal probe records and supports the view that plasma breakup or disruption was occurring in the railgun.

The induced emf of the transverse probe is shown in Figure 19. Since the emf of this probe is much smaller than the emfs recorded by the other probes, the components of the magnetic field orthogonal to the orientation axis of the vertical probe and the components of the current density orthogonal to the orientation axis of the transverse probe are small and hence can be neglected when determining the size of the Lorentz force acting on the plasma-projectile system.

4.5 Other Diagnostic Measurements

The breech voltage record for MRAP08 is shown in Figure 20. In contradiction to the results of the previous sections, the fluctuations in the record indicate that the plasma armature was unstable between $t \simeq 0.05$ and 0.35 ms [2]. Unfortunately, the muzzle voltage was not recorded in this firing. It would have probably shown the plasma disruption because when plasma disruption occurred in an RPIP firing, it appeared on both muzzle and breech voltage records [2].

The muzzle voltage record for MRAP05 is shown in Figure 21. The fluctuations between $t \simeq 0.05$ and 0.2 ms are an indication of substantial plasma leakage according to Reference [2]. The oscillations in the plateau region between $t = 0.25$ and 0.4 ms indicate that plasma disruption or instability occurred in this firing.

The muzzle voltage record for MRAP02 is shown in Figure 22. This reveals that plasma leakage also occurred early in this firing but unlike Figure 20, the amount of plasma leakage was not substantial. A region of plasma instability occurs between $t \simeq 0.2$ and 0.35 ms in Figure 22. It is probable that this instability affected the induced emf measurements of the central longitudinal and vertical probes for MRAP02. It is worth noting that the muzzle and breech indications of plasma leakage accord with the observations given in Table 2.

5. CONCLUSION

The experimental results obtained from the MRAP series are presented in this technical note. In addition to presenting the usual diagnostic measurements such as breech and muzzle voltage records, the induced emf results produced by solenoidal probes or coils in different orientations and positions along a RAPID railgun are presented.

The results of image analyses of the streak films for MRAP02, MRAP05 and MRAP08 are also presented. These results indicate that much plasma leakage occurred in MRAP02 and MRAP05 and are in accordance with the behaviour observed on the corresponding muzzle and breech voltage records. However, even though indications of plasma disruption appear on the muzzle and breech voltage records for MRAP02, MRAP05 and MRAP08, the light intensity profiles obtained from the image analyses do not show large variations in intensity number within the plasma armature. These would be expected when plasma disruption occurs. Plasma disruption might not have been detected by image analysis because the streak films could have been over-exposed.

Further work is required before the data obtained from the probes can be used to infer rail and plasma armature current distributions; i.e. to meet the first two aims of the MRAP series. The comparison of the probe data with theoretical predictions for the induced emf of the longitudinal probes is complicated because the plasma-armature was well-behaved in only one of the MRAP firings (MRAP08). Thus different models for the plasma current distribution need to be considered for the comparison to be undertaken.

6. ACKNOWLEDGEMENTS

The author wishes to thank Messrs J. Ferrett, W.A. Jenkins and D.F. Stainsby for conducting the MRAP experiments and providing the experimental data presented in this technical note.

7. REFERENCES

1. Bedford, A.J., Clark, G.A. and Thio, G.A. (1983). "Experimental Electromagnetic Launchers at MRL", MRL Technical Report MRL-R-894.

2. Kowalenko, V. "Analysis of a Series of Electromagnetic Launcher Firings", MRL Technical Report in preparation.

3. Clark, G.A. and Bedford, A.J. (1984) "Performance Results of a Small-Calibre Electromagnetic Launcher", MRL Technical Report MRL-R-917.

4. Stainsby, D.F. and Bedford, A.J. (1984) "Some Diagnostic Interpretations from Railgun Plasma Profile Experiments", IEEE Transactions on Magnetics Vol. MAG-20, No. 2, p. 332.

5. Kennett, S.R. (1984) "The Interactive Plotting Program - GRAPH", MRL Technical Note MRL-TN-485.

6. Sadedin, D.R. and Stainsby, D.F. "Experiments With a Small Injected Railgun", MRL Technical Report in preparation.

TABLE 1

Inductance and Resistance Values for the Probes in the MRAP series (Values of the Inductance and Resistance are accurate to ten and one percent respectively)

Coil	Inductance ($\times 10^{-7}$H)	Resistance (mΩ)
BC1	8.2	636
BC2	8.4	616
BC3	9.3	648
CC1	9.6	721
CC2	8.0	597
CC3	8.8	617
MCT	9.4	631
MC1	8.2	647
MC2	9.3	679
MC3	7.9	1066

TABLE 2

Firing Durations, Streak Film Observations and Exit Velocity Estimates for the MRAP Series

MRAP Firing	Duration of Firing ($\times 10^{-4}$ s)	Streak Film Observations	Exit Velocity Estimates ($\times 10^{3}$ m/s)
1	(7.3 ± 0.3)	Some plasma leakage	(1.13 ± 0.03)
2	(7.3 ± 0.3)	Some plasma leakage and separation	(1.18 ± 0.05)
3	(6.9 ± 0.5)	Over-exposed	(1.15 ± 0.05)
4	No data	Some plasma leakage, streak not continuous	--
5	(7.1 ± 0.3)	Much plasma leakage	(1.23 ± 0.03)
6	No data	No streak film obtained	--
7	(7.1 ± 0.3)	Much plasma leakage	(1.12 ± 0.03)
8	(6.6 ± 0.5)	No plasma leakage	(1.14 ± 0.05)
9	(7.2 ± 0.3)	Much plasma leakage	--

TABLE 3

Image Analysis Results for MRAP02

Time (μs)	Position (mm)	Plasma Length (mm)
12 ± 7	55 ± 8	20 ± 2
38 ± 7	74 ± 5	72 ± 3
58 ± 8	74 ± 5	71 ± 3
94 ± 8	79 ± 7	80 ± 3
108 ± 9	80 ± 7	80 ± 3
120 ± 9	86 ± 7	85 ± 3
135 ± 9	93 ± 7	92 ± 3
145 ± 9	96 ± 7	92 ± 3
164 ± 10	98 ± 7	92 ± 3
200 ± 11	124 ± 7	116 ± 4
209 ± 11	127 ± 7	118 ± 4
220 ± 11	127 ± 7	118 ± 4
234 ± 11	132 ± 7	124 ± 4
262 ± 12	147 ± 7	128 ± 4
279 ± 12	151 ± 7	118 ± 4
292 ± 12	158 ± 7	114 ± 4
294 ± 13	154 ± 6	116 ± 4
309 ± 13	168 ± 8	122 ± 4
327 ± 13	171 ± 8	123 ± 4
348 ± 14	183 ± 8	126 ± 4
361 ± 14	193 ± 8	128 ± 4
384 ± 15	212 ± 8	125 ± 4
408 ± 15	226 ± 8	118 ± 4
440 ± 16	251 ± 8	121 ± 4
463 ± 16	273 ± 8	127 ± 4
482 ± 17	289 ± 9	135 ± 4
510 ± 17	311 ± 8	139 ± 4
532 ± 18	347 ± 9	141 ± 4
560 ± 18	354 ± 9	143 ± 4
583 ± 19	358 ± 9	146 ± 4
591 ± 19	388 ± 7	145 ± 5
624 ± 20	410 ± 7	142 ± 5
646 ± 21	432 ± 8	145 ± 5
665 ± 21	450 ± 8	145 ± 5
682 ± 21	460 ± 8	138 ± 5
701 ± 22	485 ± 9	128 ± 9
720 ± 22	493 ± 9	129 ± 5

TABLE 4

Image Analysis Results for MRAP05

Time (μs)	Position (mm)	Plasma Length (mm)
3 ± 4	49 ± 3	4 ± 2
16 ± 4	61 ± 3	28 ± 3
22 ± 5	63 ± 3	36 ± 3
34 ± 5	69 ± 3	50 ± 3
50 ± 6	69 ± 5	55 ± 3 or 70 ± 3
67 ± 6	72 ± 5	57 ± 3 or 70 ± 3
87 ± 7	77 ± 5	81 ± 4
103 ± 8	78 ± 5	80 ± 4
116 ± 9	77 ± 5	79 ± 4
134 ± 10	90 ± 5	93 ± 4
150 ± 10	117 ± 6	117 ± 4
162 ± 11	133 ± 6	131 ± 5
175 ± 12	144 ± 7	142 ± 5
198 ± 13	130 ± 6	110 ± 4
211 ± 13	144 ± 6	124 ± 5
230 ± 14	167 ± 7	145 ± 5
245 ± 15	156 ± 7	135 ± 5
254 ± 15	165 ± 7	145 ± 5
265 ± 16	180 ± 7	157 ± 5
273 ± 16	188 ± 7	167 ± 6
277 ± 17	181 ± 7	161 ± 5
290 ± 18	168 ± 7	147 ± 5
305 ± 18	180 ± 7	156 ± 5
315 ± 18	188 ± 7	161 ± 5
346 ± 21	237 ± 8	142 ± 5
366 ± 21	231 ± 8 or 259 ± 9	185 ± 7 or 213 ± 8
379 ± 22	214 ± 8 or 243 ± 8	167 ± 7 or 190 ± 8
399 ± 23	231 ± 8 or 246 ± 8	148 ± 6 or 164 ± 7
421 ± 24	246 ± 8	153 ± 7
427 ± 24	239 ± 8	139 ± 7
436 ± 25	256 ± 9	144 ± 7
452 ± 25	259 ± 9	148 ± 7
453 ± 24	279 ± 7	176 ± 7
465 ± 25	290 ± 7	181 ± 7
474 ± 25	290 ± 7	178 ± 7
489 ± 26	299 ± 7	172 ± 7
505 ± 27	311 ± 8	178 ± 7
513 ± 27	348 ± 8	175 ± 7
526 ± 28	367 ± 9	186 ± 7
535 ± 28	376 ± 9	190 ± 8
597 ± 31	378 ± 9	195 ± 8
606 ± 32	392 ± 9	184 ± 8
613 ± 32	409 ± 10	200 ± 8
645 ± 33	440 ± 10	221 ± 8
661 ± 34	455 ± 11	234 ± 9
676 ± 35	460 ± 11	210 ± 8
691 ± 36	475 ± 11	206 ± 8

TABLE 5

Image Analysis Results for MRAP08

Time (μs)	Position (mm)	Plasma Length (mm)
2 ± 2	53 ± 7	17 ± 3
18 ± 14	53 ± 7	19 ± 3
30 ± 14	63 ± 8	44 ± 3
42 ± 4	65 ± 8	62 ± 4
56 ± 5	66 ± 8	62 ± 4
68 ± 5	66 ± 8	64 ± 4
83 ± 6	67 ± 8	65 ± 4
95 ± 6	73 ± 8	70 ± 4
113 ± 7	76 ± 9	73 ± 4
138 ± 7	82 ± 9	79 ± 4
161 ± 8	88 ± 9	77 ± 4
176 ± 8	87 ± 9	78 ± 4
177 ± 9	96 ± 9	79 ± 4
196 ± 9	108 ± 10	83 ± 4
201 ± 9	108 ± 10	83 ± 4
207 ± 10	113 ± 10	82 ± 4
209 ± 9	113 ± 10	84 ± 4
221 ± 10	117 ± 10	81 ± 4
224 ± 10	118 ± 10	81 ± 4
227 ± 10	120 ± 10	81 ± 4
234 ± 10	122 ± 10	82 ± 4
241 ± 11	124 ± 10	78 ± 4
254 ± 11	131 ± 10	77 ± 4
259 ± 11	133 ± 10	76 ± 4
261 ± 11	134 ± 10	76 ± 4
276 ± 12	142 ± 10	75 ± 4
294 ± 12	156 ± 11	77 ± 4
306 ± 12	165 ± 11	77 ± 4
343 ± 14	186 ± 11	70 ± 4
356 ± 14	193 ± 11	67 ± 4
378 ± 15	211 ± 12	66 ± 4
401 ± 16	236 ± 13	63 ± 4
413 ± 16	240 ± 13	64 ± 4
433 ± 16	258 ± 13	66 ± 4
453 ± 17	271 ± 13	62 ± 4
467 ± 18	282 ± 14	64 ± 4
486 ± 18	305 ± 14	69 ± 4
506 ± 19	325 ± 15	78 ± 4
526 ± 19	347 ± 15	89 ± 4
539 ± 20	358 ± 15	93 ± 4
552 ± 20	370 ± 16	89 ± 4
557 ± 20	371 ± 16	84 ± 4
562 ± 20	366 ± 16	86 ± 4
573 ± 21	379 ± 16	87 ± 4
584 ± 21	386 ± 16	81 ± 4
597 ± 22	401 ± 16	82 ± 4
614 ± 22	421 ± 17	90 ± 4
639 ± 23	450 ± 18	102 ± 5
653 ± 23	463 ± 18	107 ± 5
672 ± 24	481 ± 18	111 ± 5
692 ± 24	504 ± 19	114 ± 5

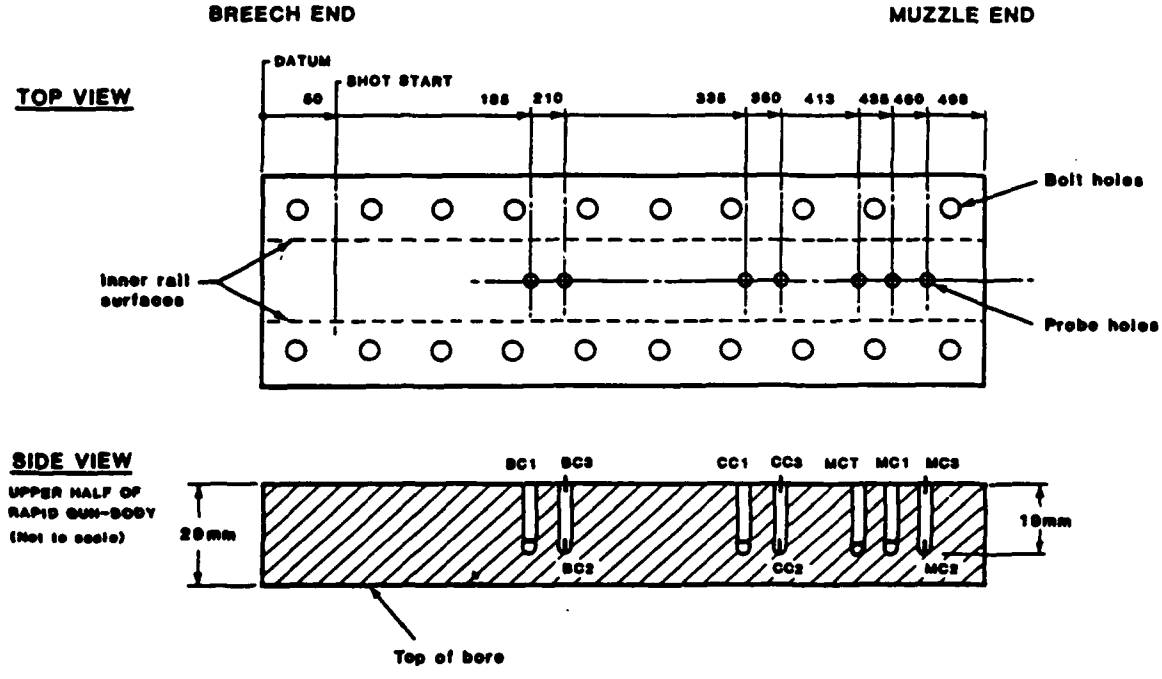

FIGURE 1 Probe locations for the MRAP series.

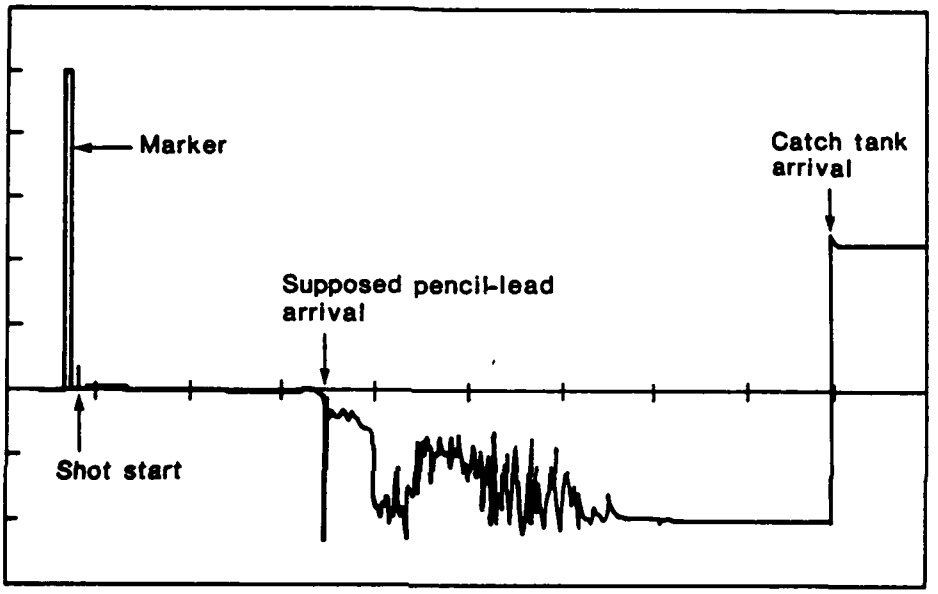

FIGURE 2 Time-of-arrival record for MRAP08.

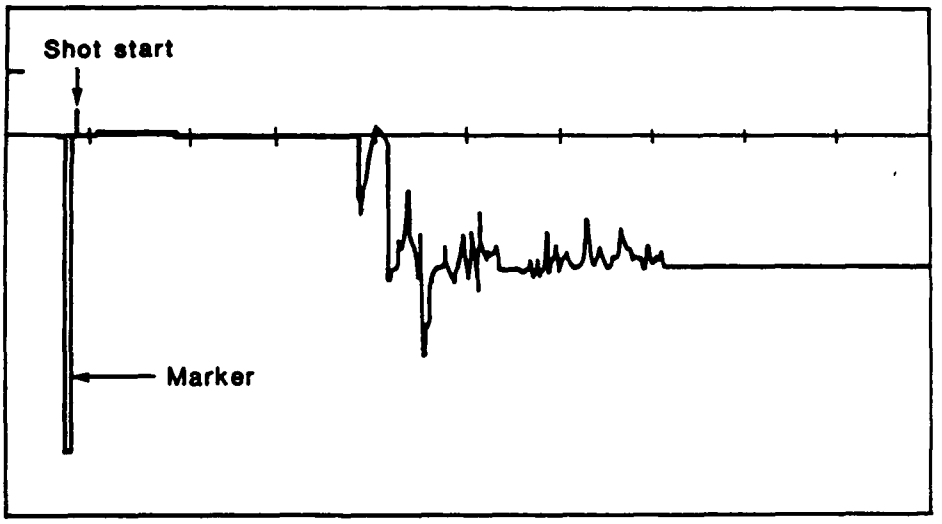

FIGURE 3 Time-of-arrival record for MRAP09.

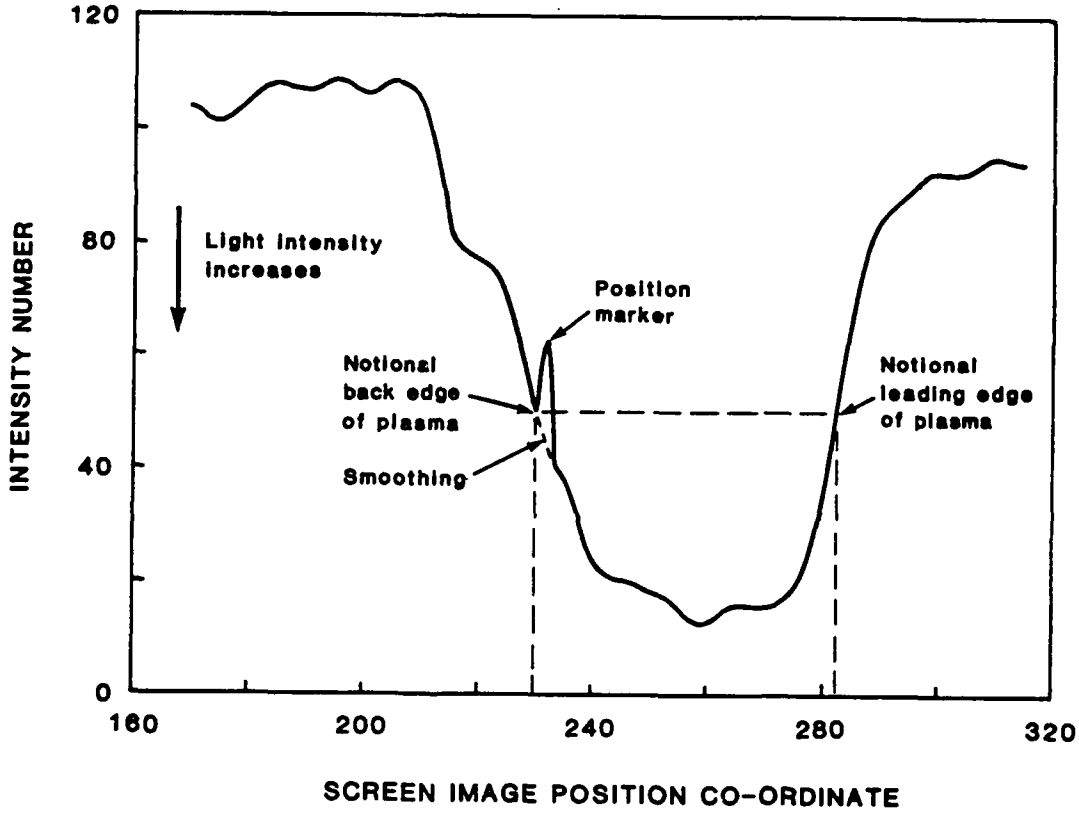

FIGURE 4 Plasma intensity profile for MRAP02 at 327 ± 13 μs after shot-start.
Plasma length = 123 ± 4 mm.
Position of the plasma leading edge from the breech = 171 ± 8mm.

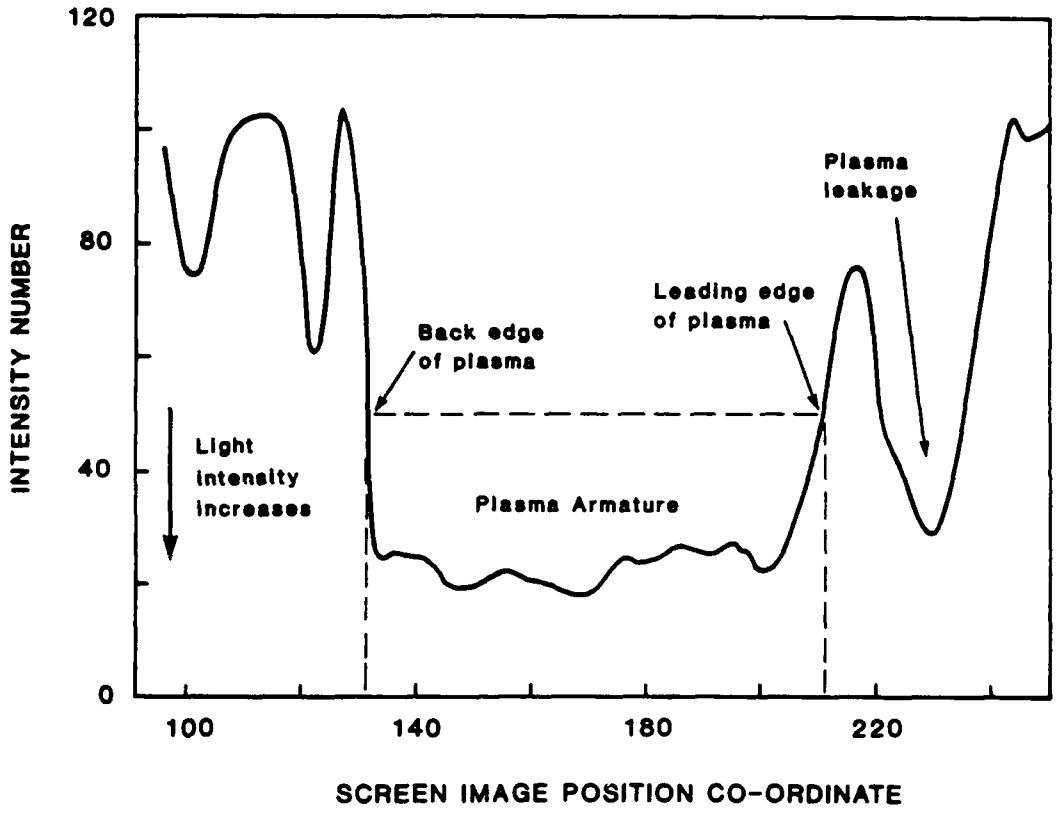

FIGURE 5 Plasma intensity profile for MRAP05 at 211 ± 13 μs after shot-start.
Plasma length = 124 ± 5 mm.
Position of the plasma leading edge from the breech = 144 ± 6mm.

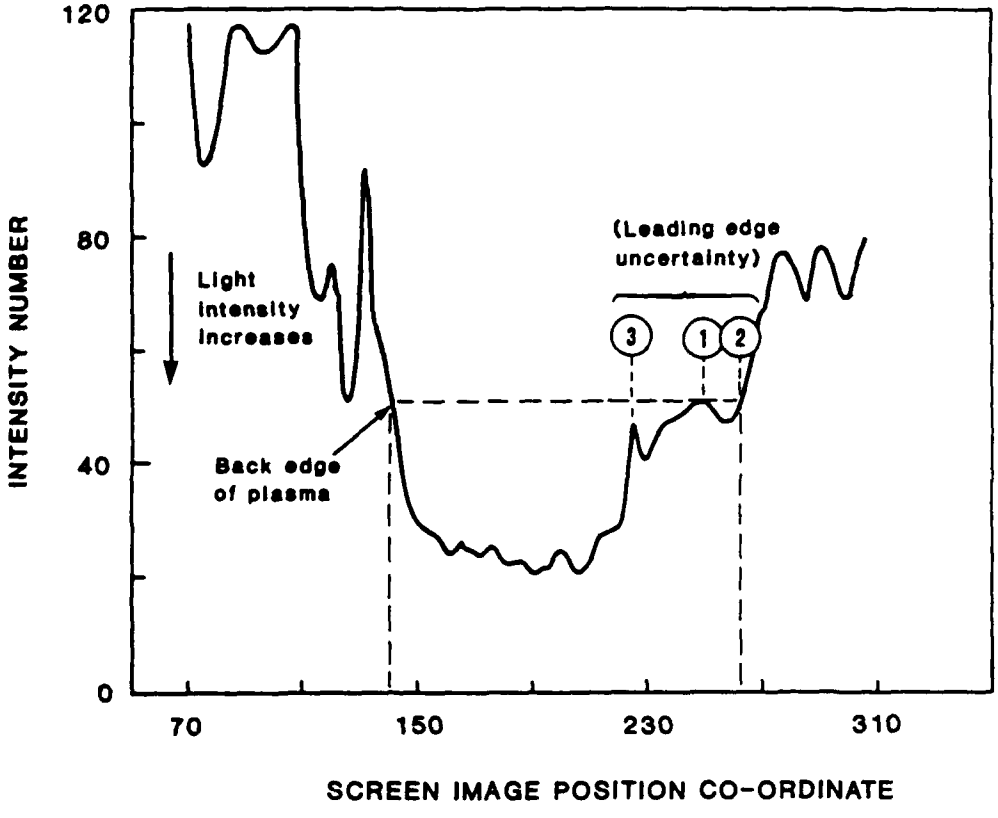

FIGURE 6 Plasma intensity profile for MRAP05 at 366 ± 21 μs after shot-start.
Plasma length = 185 ± 7 or 213 ± 8 mm.
Position of the plasma leading edge from the breech = 231 ± 8 or 259 ± 9 mm.

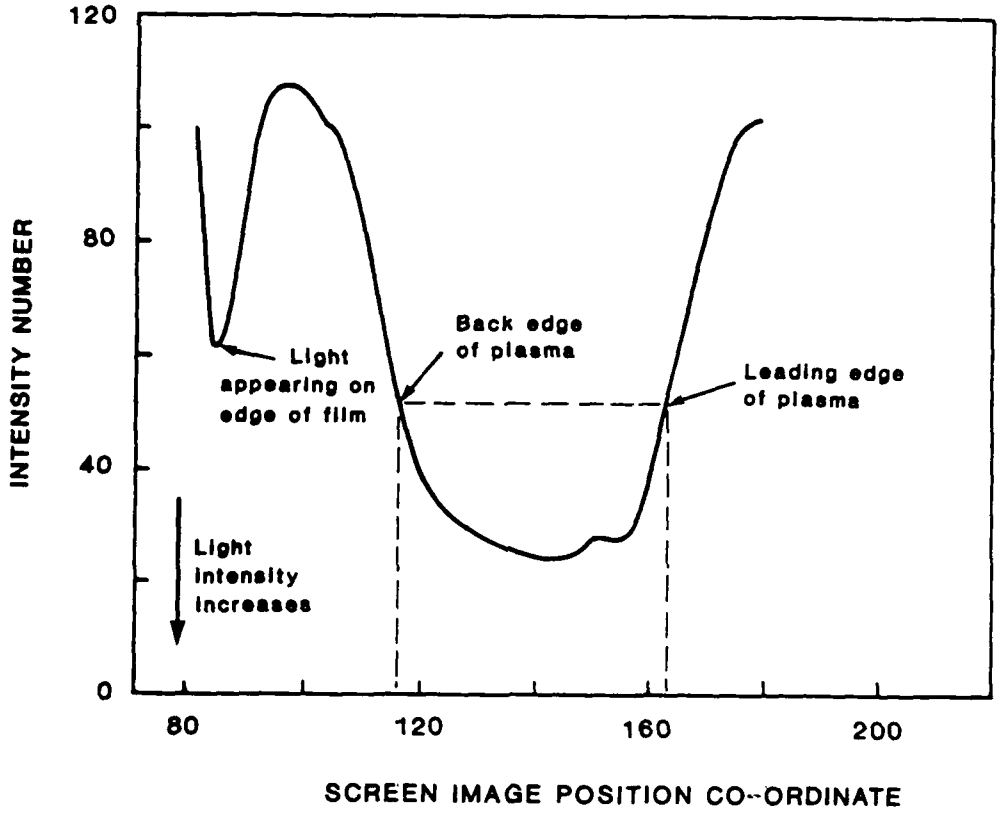

FIGURE 7 Plasma Intensity Profile for MRAP08 at 241 ± 11 μs after shot-start.
Plasma Length = 78 ± 4 mm.
Position of the plasma leading edge from the breech = 124 ± 10mm

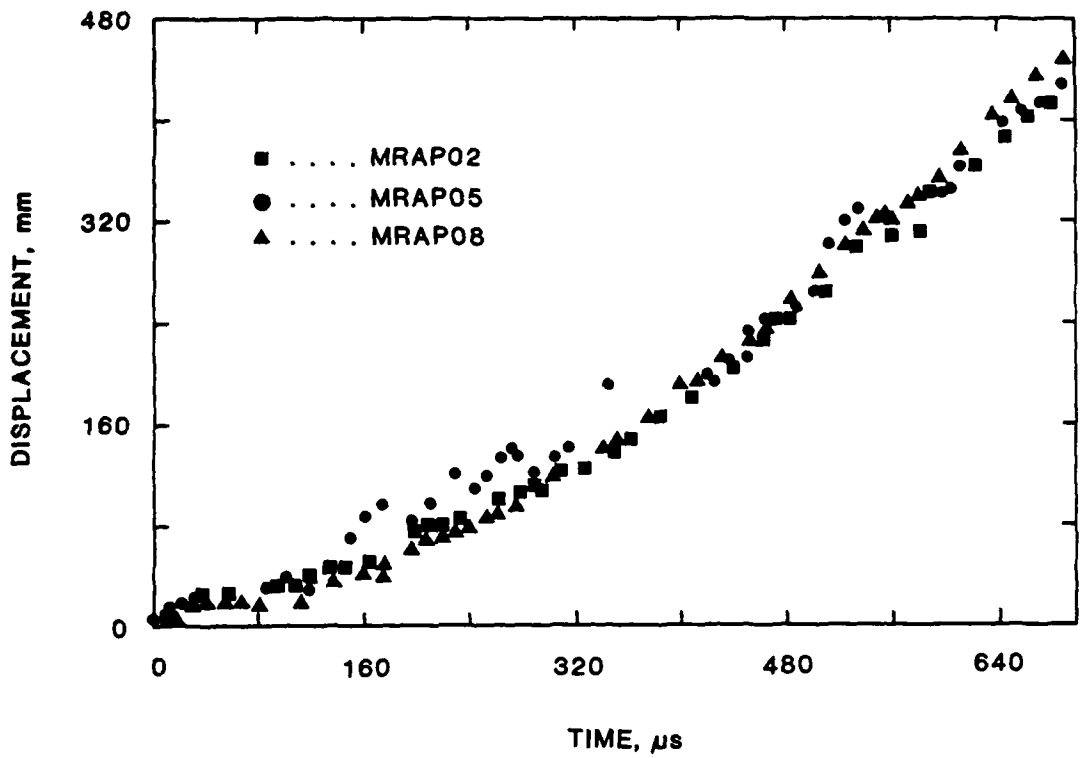

FIGURE 8 Displacement of plasma leading-edge vs time.

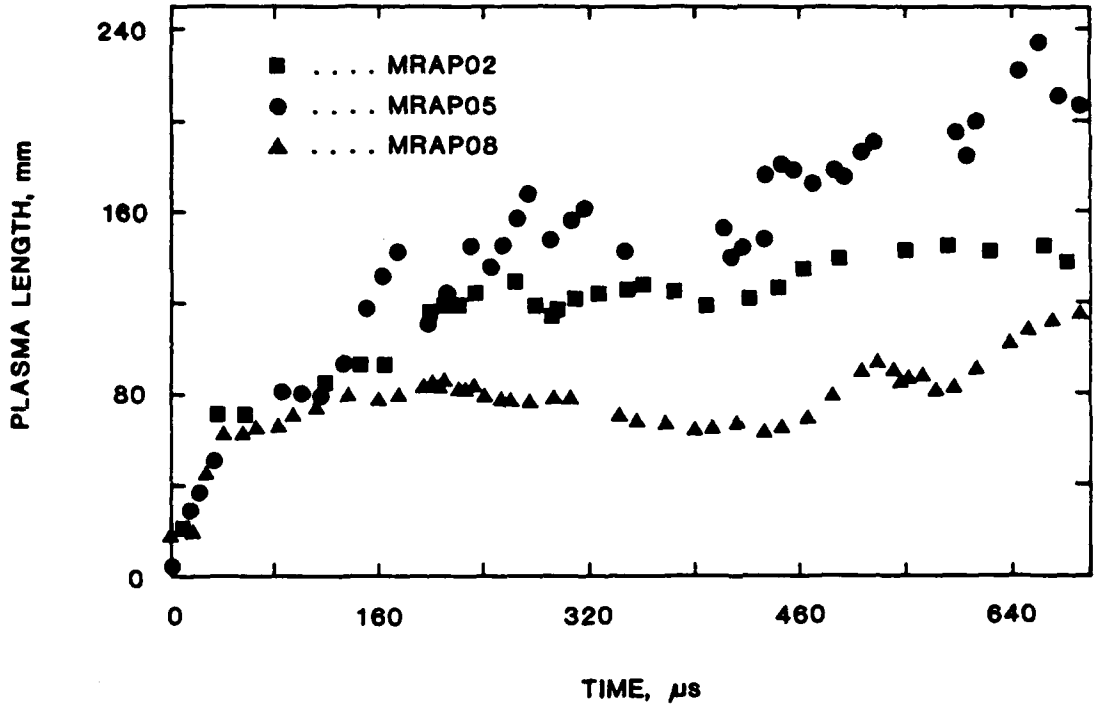

FIGURE 9 Plasma length vs time.

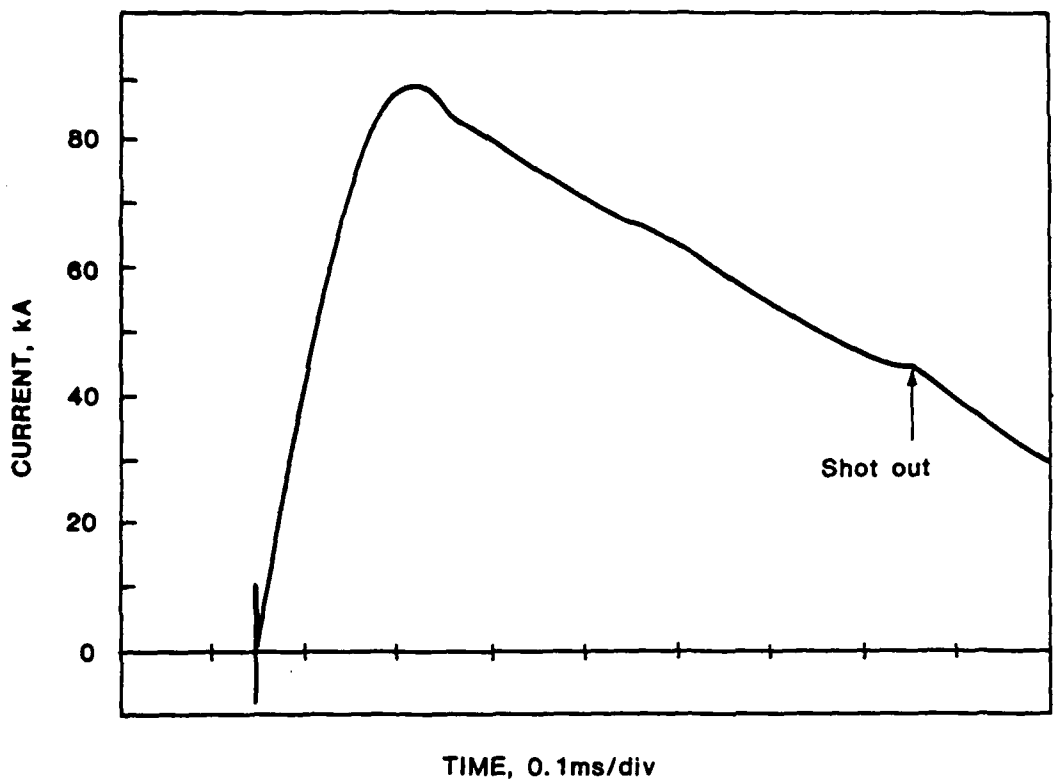

FIGURE 10 Current-time record for MRAP08.

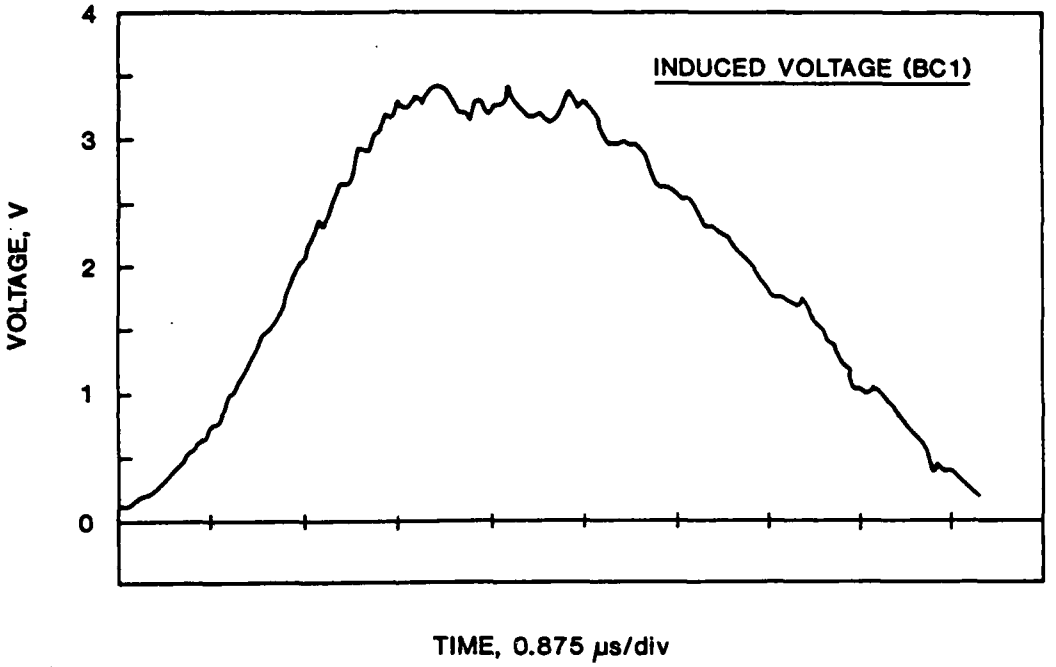

FIGURE 11 Induced emf of the vertical probe situated 185 mm from to the breech for MRAP05.

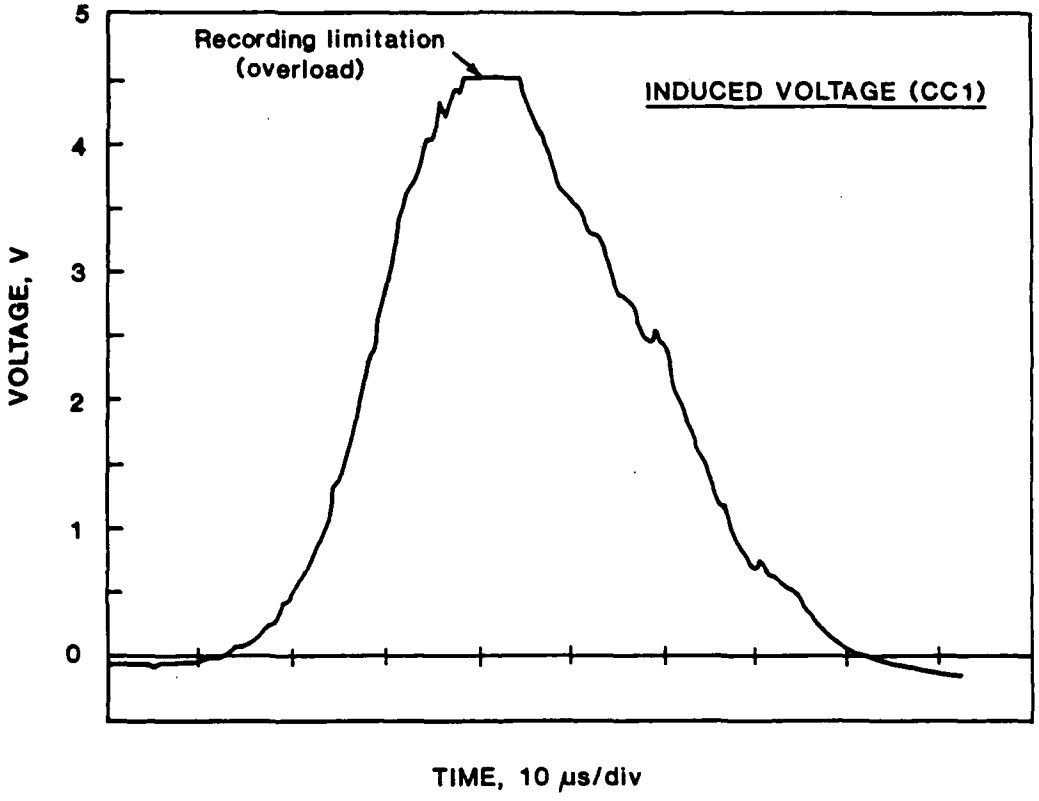

FIGURE 12 Induced emf of the vertical probe situated 335 mm from the breech for MRAP08.

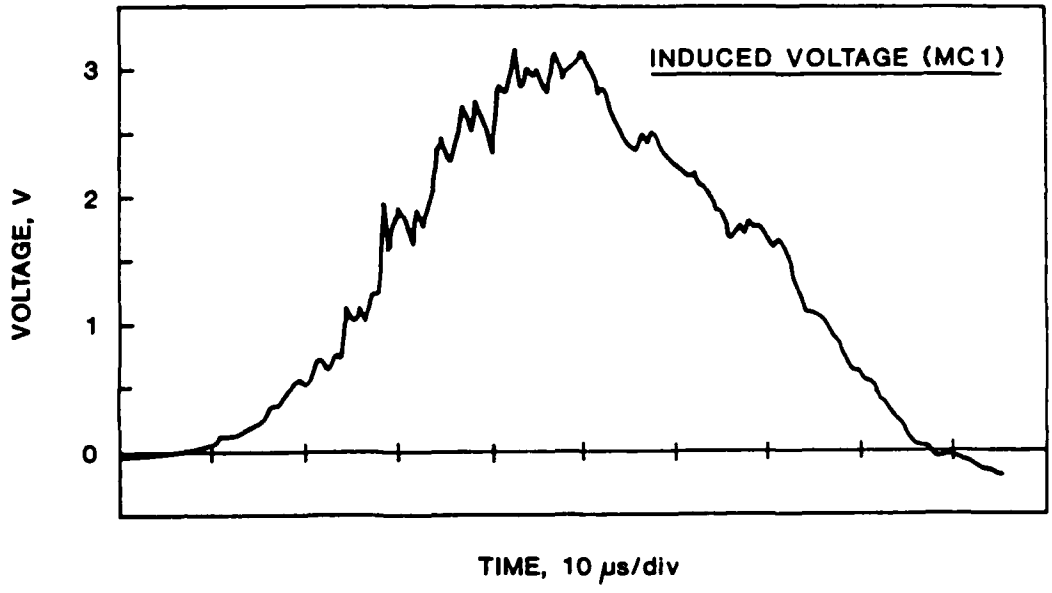

FIGURE 13 Induced emf of the vertical probe situated 435 mm from the breech for MRAP08.

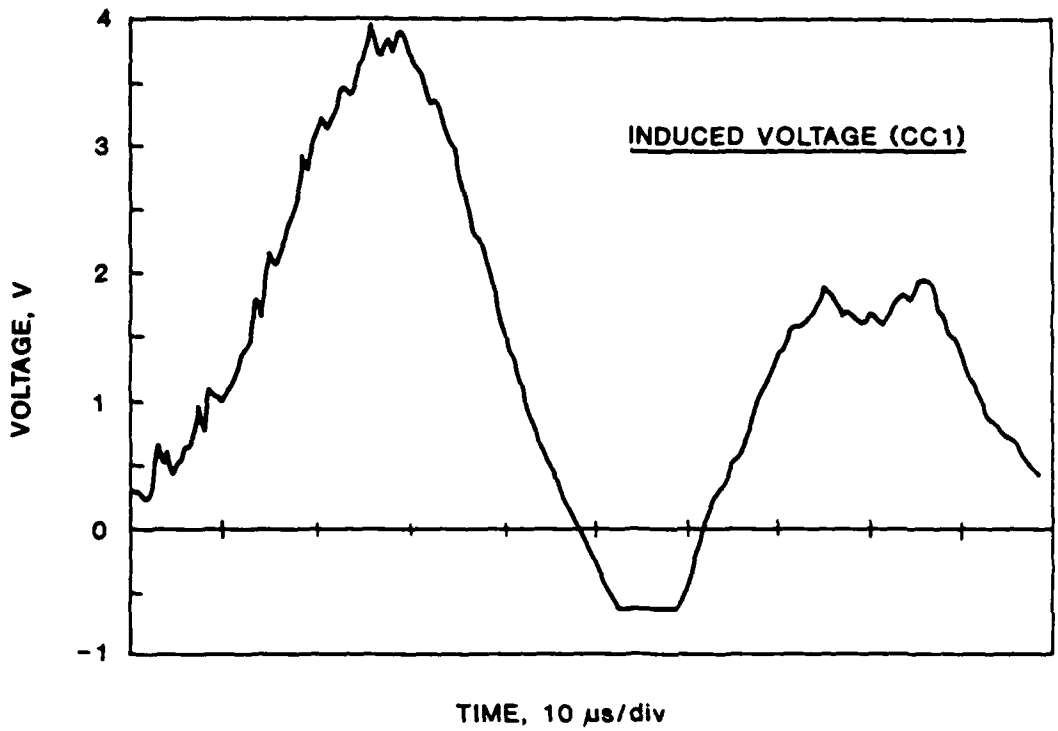

FIGURE 14 Induced emf of the vertical probe situated 335 mm from the breech for MRAP02.

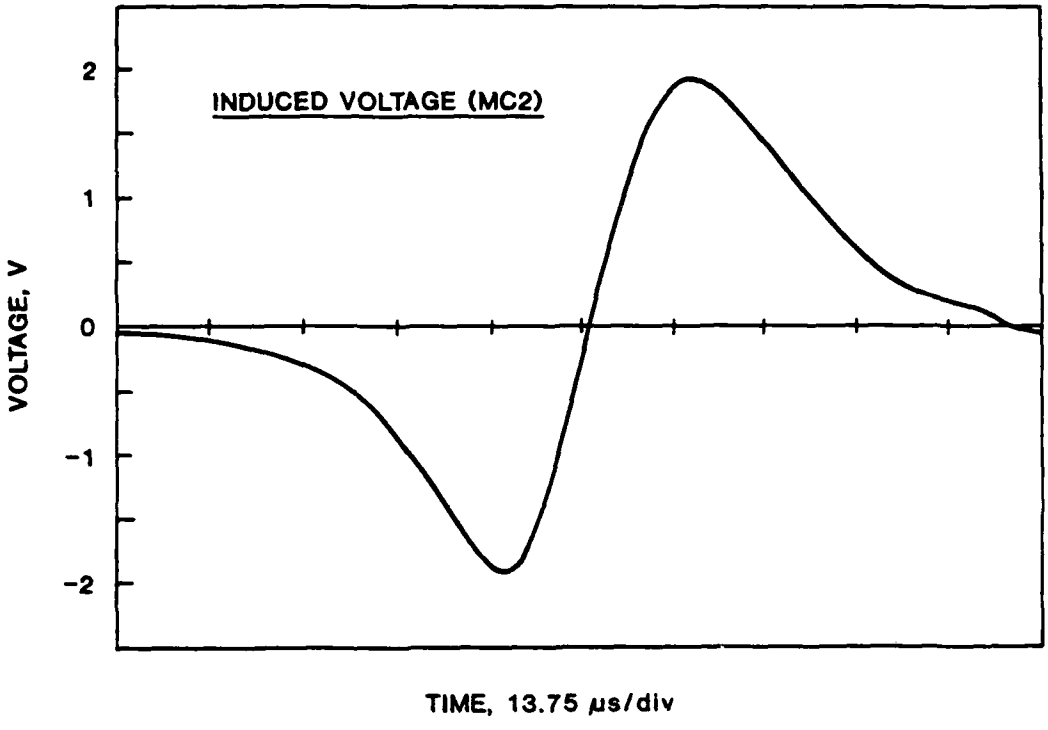

FIGURE 15 Induced emf of a longitudinal probe for MRAP08 situated 460 mm from the breech.

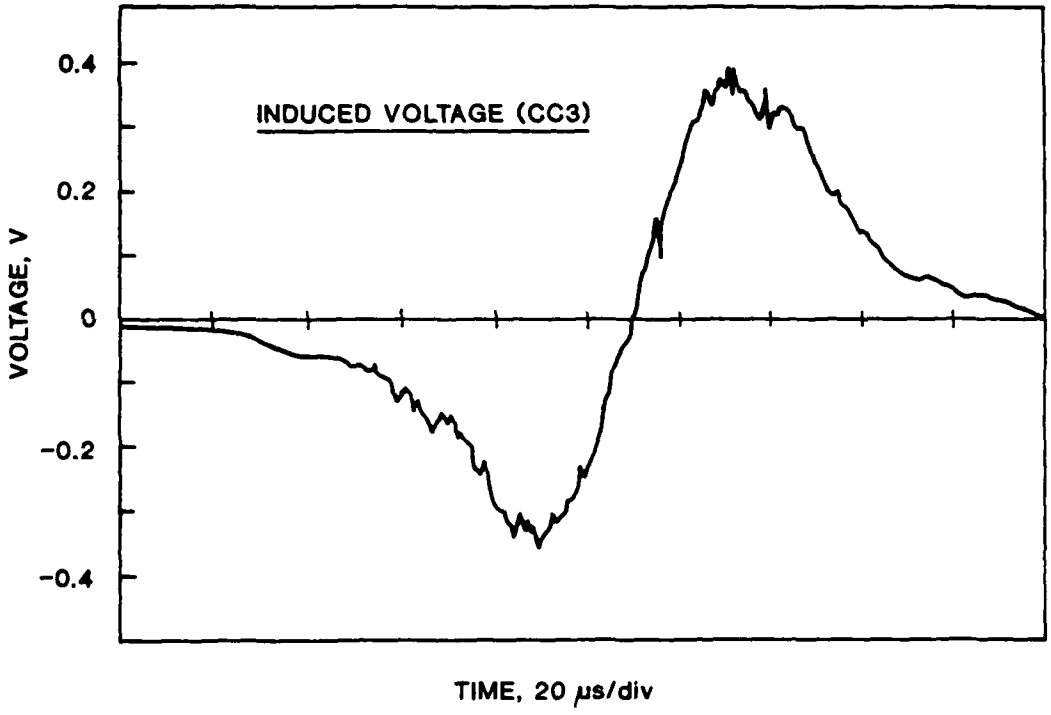

FIGURE 16 Induced emf of a longitudinal probe for MRAP09 situated 360 mm from the breech.

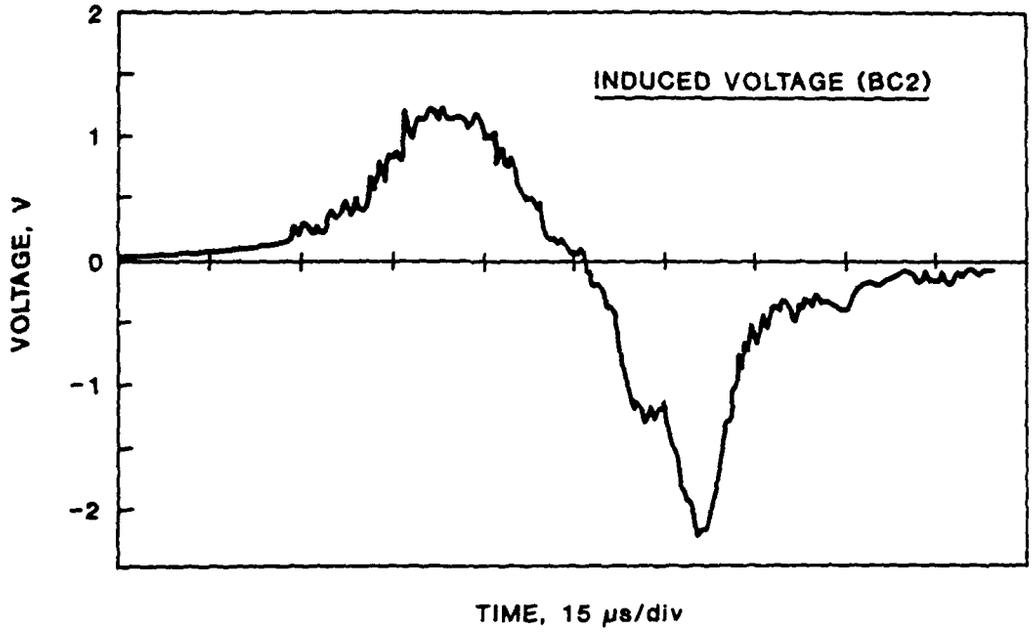

FIGURE 17 Induced emf of a longitudinal probe for MRAP09 situated 210 mm from the breech.

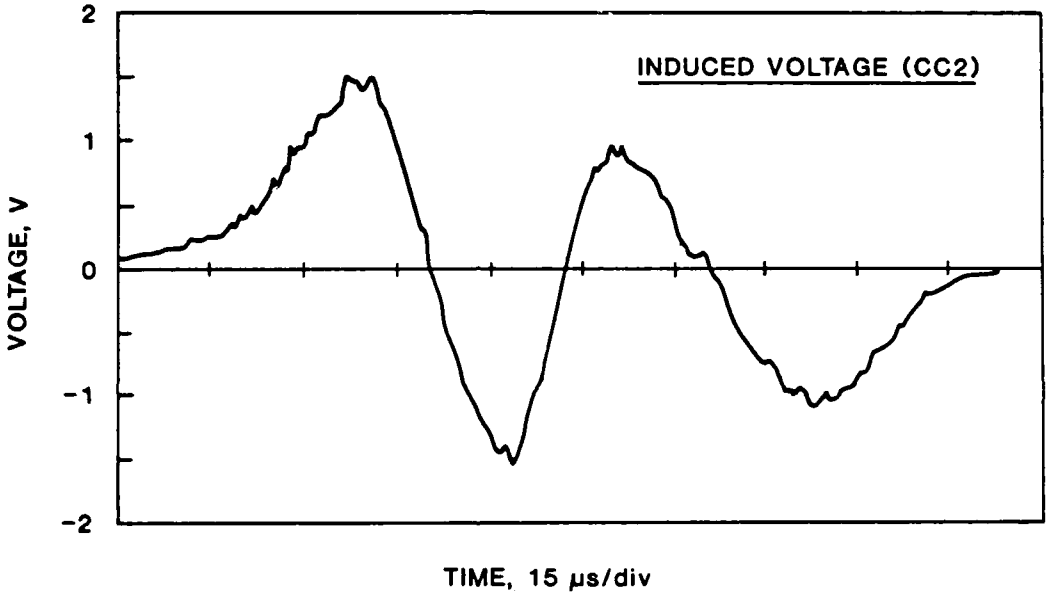

FIGURE 18 Induced emf of a longitudinal probe situated 360 mm from the breech for MRAP02.

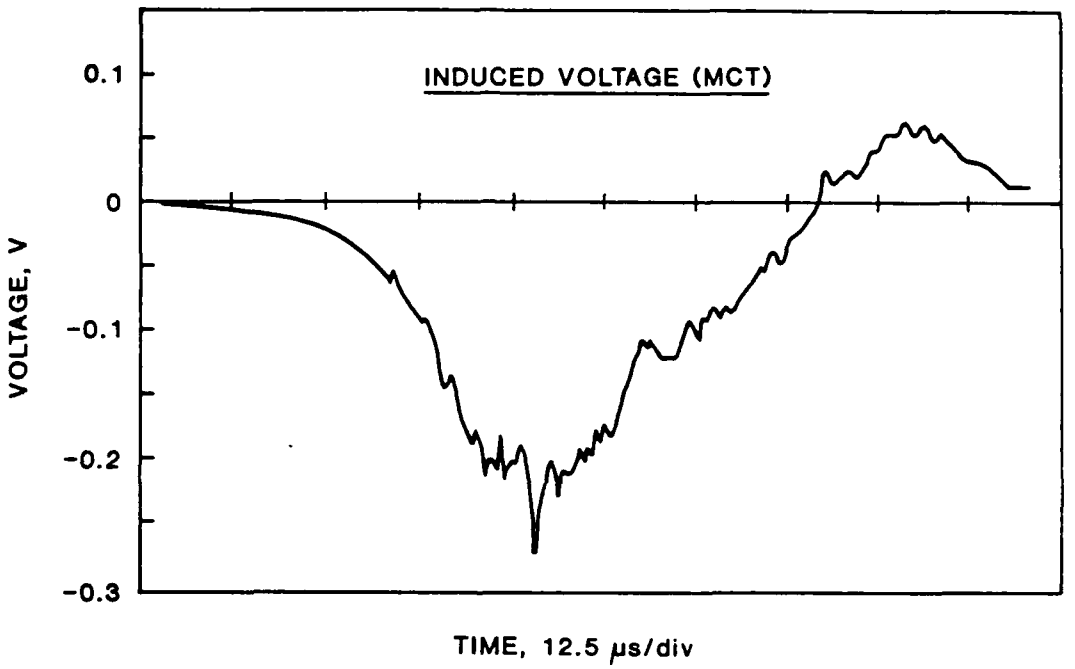

FIGURE 19 Induced emf of the transverse probe for MRAP05 situated 413 mm from the breech.

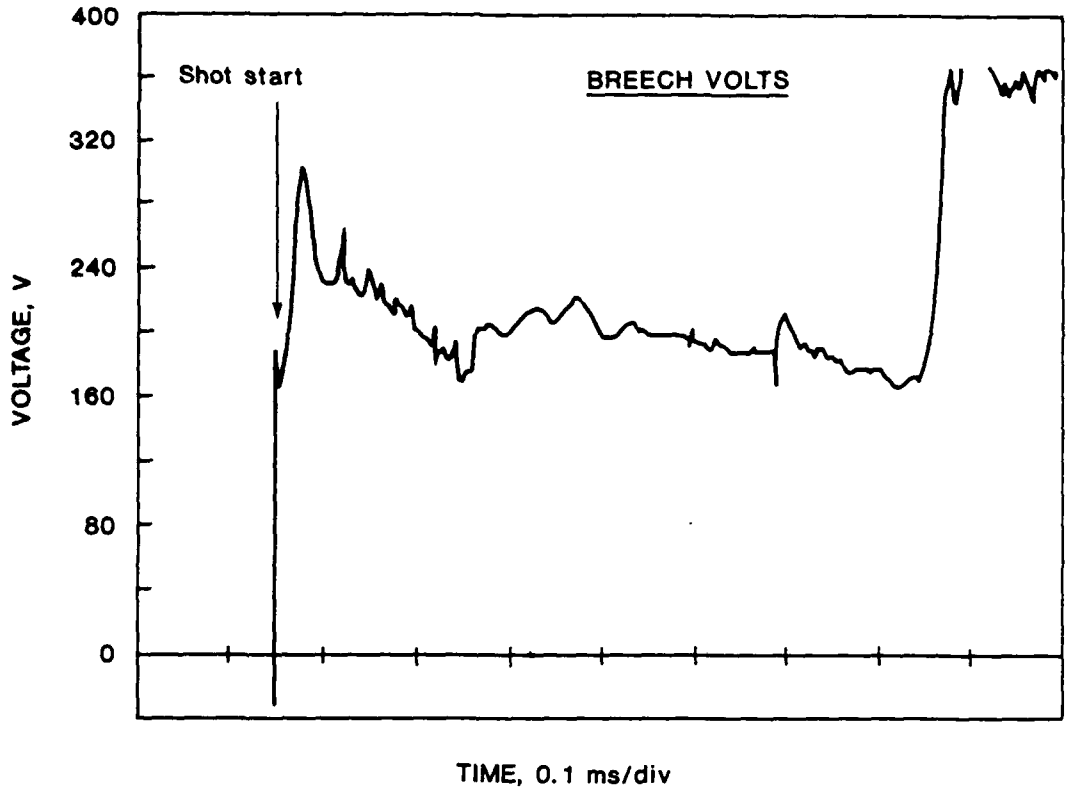

FIGURE 20 Breech voltage record for MRAP08.

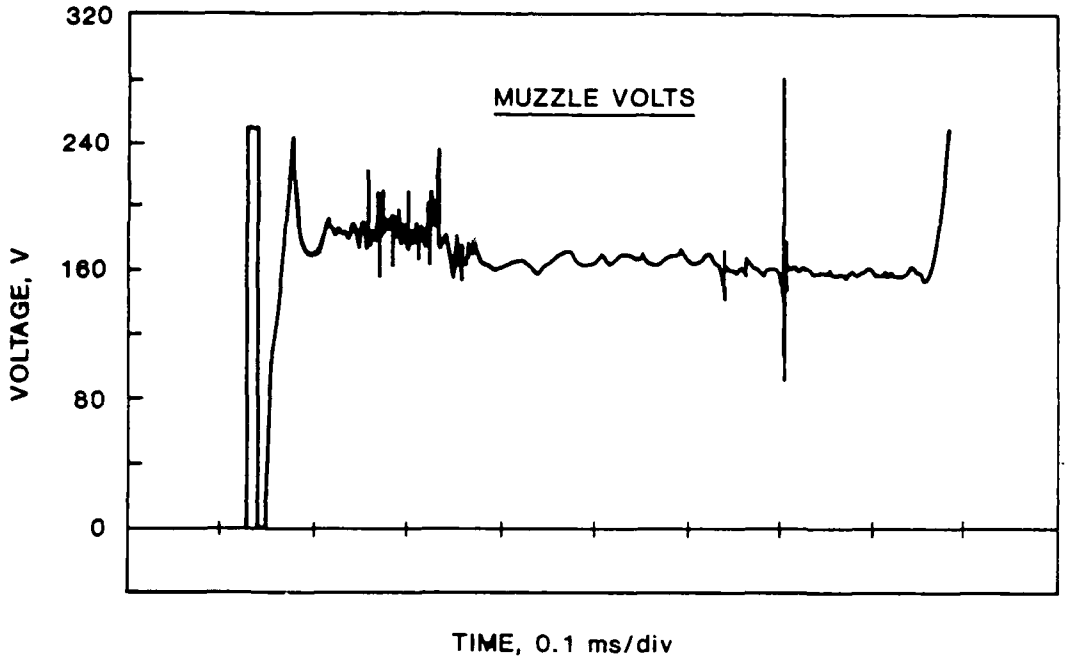

FIGURE 21 Muzzle-voltage record for MRAP05.

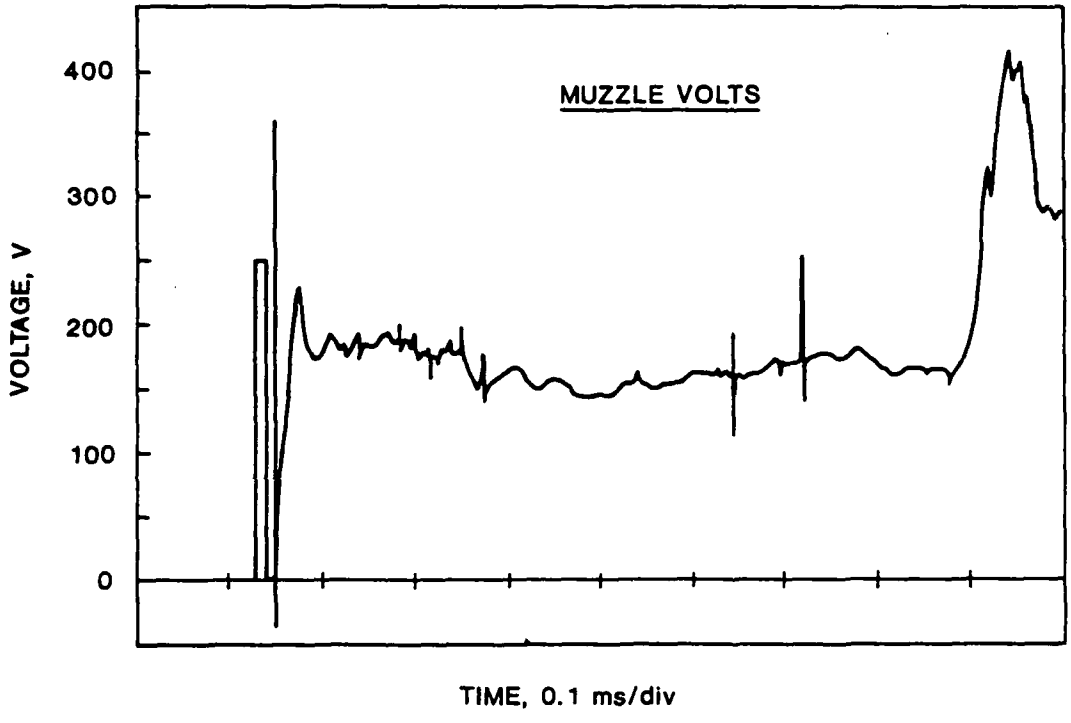

FIGURE 22 Muzzle voltage record for MRAP02.